

# ELECTRON CLOUD BUILD-UP IN TWO-BEAM REGIONS FOR HL-LHC: HEAT LOAD AND VACUUM ASPECTS

G. Skripka\*, G. Iadarola, CERN, 1211 Geneva, Switzerland

## Abstract

Electron cloud in particle accelerators is known to have a detrimental effect on the vacuum pressure and can cause a large heat deposition on a vacuum chamber surface. In a particle collider, in the presence of two beams in the same chamber, the build-up of the electron cloud becomes more complicated and the electron density cannot be simply scaled from the case of a single beam. The build-up process in the devices with common chambers can be modeled by correctly accounting for the arrival times of the two beams, the beam positions and their sizes. Numerical studies were made to estimate the electron flux on the internal surfaces of two common chamber devices of the future High Luminosity Large Hadron Collider: the triplet assemblies in the four experimental insertion regions and the injection protection absorber (TDIS). Different possible coating options in both devices were investigated aiming at a reduction of the electron current and of the deposited heat load.

## INTRODUCTION

The operation of the Large Hadron Collider (LHC) with 25 ns bunch spacing during Run 2 has shown that beam induced heat loads can pose serious limitations on the achievable machine performance [1,2]. One of the main sources of the beam-induced heat loads in the LHC is known to be electron cloud (e-cloud). Electrons impacting on the vacuum chamber surface introduce a thermal load additional to the one induced by the impedance and the synchrotron radiation emitted by the circulating beam. The heat loads induced by e-cloud can pose serious limitations for operation of cryogenic devices. Another limitation posed by the e-cloud is the rapid increase of the vacuum pressure above the acceptable level due to electron-stimulated gas desorption. It is therefore important to assess the potential limitations for the High Luminosity LHC (HL-LHC) era [3] when the machine will operate with the 25 ns bunch spacing and double bunch intensity with respect to the present configuration. In the studies presented here we used the PyE-CLOUD code, which allows simulating the e-cloud build-up in the presence of one or multiple circulating beams in one chamber [4]. The employed modelling of the secondary emission process is described in [5]. In the following we will call "SEY parameter" the maximum of the SEY curve.

### *Simulating the e-cloud buildup with two beams in the same chamber*

Numerical simulations of the e-cloud build-up in devices with a common chamber require special care [5–7]. The arrival time of bunches from the two beams depends on the

position along the device, hence, there is not a simple bunch spacing describing the time structure of the beams.

Due to the non-linearity in the e-cloud build-up mechanism, the electron density cannot be simply scaled from the case of the single beam and the build-up process in the devices with common chambers has to be modelled correctly accounting for the arrival times of the two beams, their position and their size at different location along the device.

For the case of two beams in a common chamber the e-cloud densities from beam 1 and beam 2 separately do not add up to the total density for the two beams simultaneously in the chamber and that also the multipacting threshold is different. When simulating the two beams together, the delay in the arrival time plays a significant role. In particular, we should point out that the multipacting is not always stronger in the presence of two beams compared to the single beam case [8].

The PyE-CLOUD code used for this simulation study is 2D code. Therefore in order to get the longitudinal e-cloud profile, slices along the device at given longitudinal positions have to be simulated, correctly accounting for the difference in the arrival time of the two beams as well as the other beam properties at each section. The LREs, where the counter-rotating beams pass simultaneously occur at evenly spaced locations along the machine. In between LREs the delay between bunch passages from the two beams range between -12.5 ns to +12.5 ns (for the nominal bunch spacing of 25 ns). We have simulated two "LHC batches" each made of 4 train of 72 bunches separated by gaps of 225 ns for both beam 1 and 2. The spacing between the batches is 800 ns.

### *Common chamber devices for HL-LHC*

One type of the common chamber device in the current LHC and future HL-LHC are the Inner Triplets installed on each side of the four experimental interaction points. The triplet assembly consists of superconducting quadrupole magnets (Q1, Q2, Q3), one separation/recombination superconducting dipole (D1), a corrector package (including sextupoles, octupoles, decapoles, dodecapoles in both normal and skew orientations) and drift spaces as sketched in Fig. 1. The reduction of the heat deposition on the cold magnets is of high importance. Therefore, the heat load was estimated for all elements of the new Inner Triplets in points 1 and 5 which are being designed for the HL-LHC project, taking into account the presence of a surface treatment (coatings) for the reduction of the SEY.

Another critical common chamber device in the HL-LHC is the TDIS injection protection absorber (Fig. 2), designed to absorb the beam injected into the LHC, in case of injection kicker malfunctions and timing errors. Two such devices will be installed: one in the common region at point 2 and one

\* galina.skripka@cern.ch

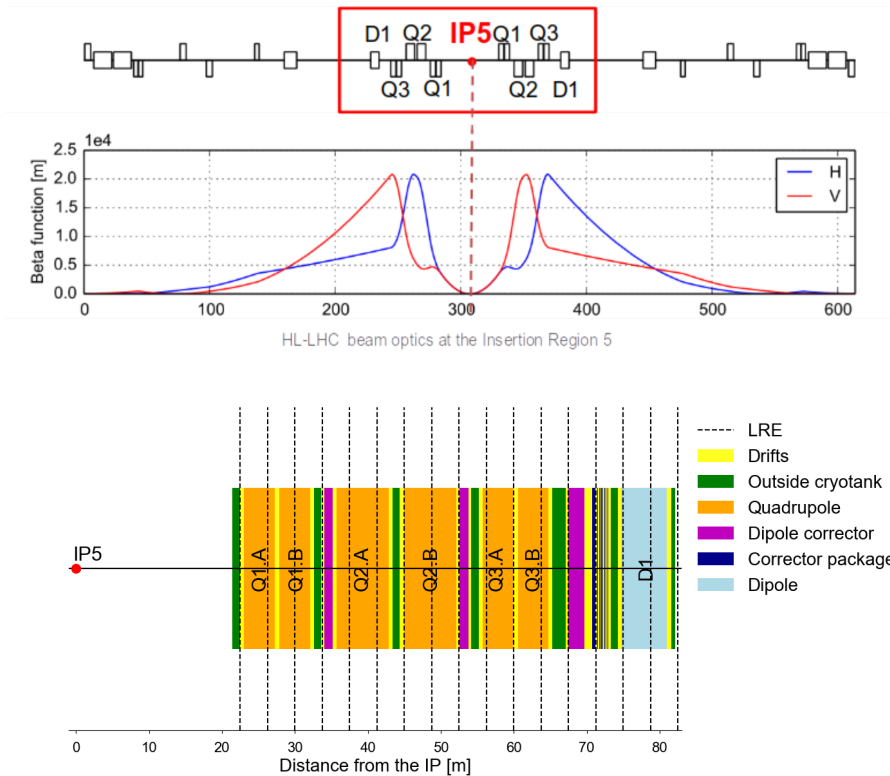


Figure 1: HL-LHC beam optics at insertion region 5 (top) and a detailed layout for the right hand side of the interaction point 5, with the LREs in the triplet marked by dashed lines (bottom).

at point 8. TDIS is designed to have three segments with movable absorbing jaws on the top and the bottom of one beam (the one that is injected right upstream of the device) and a single beam screen surrounding the second circulating beam. During the LHC operation, a similar injection protection absorber TDI has suffered from vacuum issues observed when retracting the jaws after the beam injection, as well as heating and other issues [9–11].

## E-CLOUD BUILD-UP SIMULATIONS

The main beam parameters used in the build-up simulations are reported in Table 1. The triplets were simulated with the beams at 7 TeV energy since the multipacting is expected to be stronger. For the TDIS absorber we have studied the build-up process with the 450 GeV beams, when the jaws are moved closer to the beam. After the beam injection the TDIS jaws are retracted and stay parked far from the beams.

To correctly model the two counter-rotating beams in the same chamber, we simulate different slices along the device, accounting for the different arrival times, the transverse sizes and the transverse positions of the two beams at each section. A sufficiently long portion of the beam has been simulated in order to reach the equilibrium number of electrons at all sections where multipacting occurs. All results presented in the following are re-scaled to the full number of bunches for HL-LHC.

Table 1: Simulation parameters

Energy, GeV	7000 (triplets) / 450 (TDIS)
Intensity, p/bunch	$2.2 \times 10^{11}$
RMS bunch length (Gaussian), m	0.09
Bunch spacing, ns	25
Optics	HL-LHC v1.2 ( $\beta^* = 15$ cm)

### Inner Triplets

We present the study for the Inner Triplets on the right side of the interaction point 5 (IP5) of the HL-LHC. Due to the symmetry considerations, the results are applicable to the identical devices installed on the other side and at the IP1. Also the Inner Triplets at the low-luminosity interaction points (IP2 and IP8) were simulated. The results of the study can be found in [12]. Coating with amorphous carbon (*a-C*) is foreseen for all HL-LHC Inner Triplets to reduce the heat load and avoid e-cloud-induced instabilities.

Simulations were performed for a number of sections along the triplet assembly and for different values of the SEY parameter assuming  $SEY = 1.3$  for the *uncoated case* and  $SEY = 1.1$  when the *a-C* coating of the beam screen is present. For these two cases, the heat load distributions along the Inner Triplet are compared in the left plot in Fig. 3. The dashed vertical lines mark the locations of the LREs. The heat load tends to be larger at locations between the LREs where the beams are not synchronized (effective bunch spacing of 12.5 ns). The largest peaks are observed at the

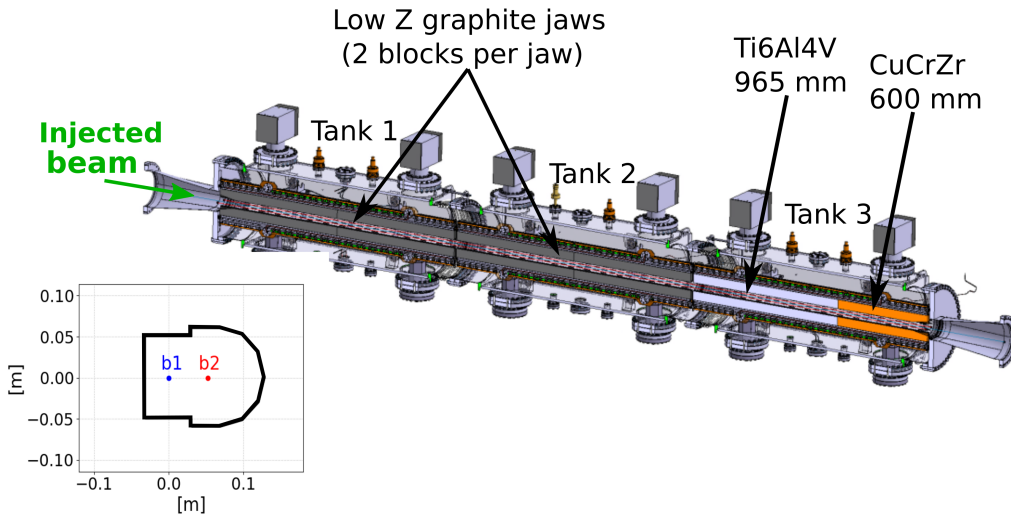


Figure 2: TDIS model with indicated the materials of the jaws (from [13]). The 2D chamber cross-section used in PyECLLOUD simulations is shown in the corner. The injected and circulating beams are indicated in blue and red respectively.

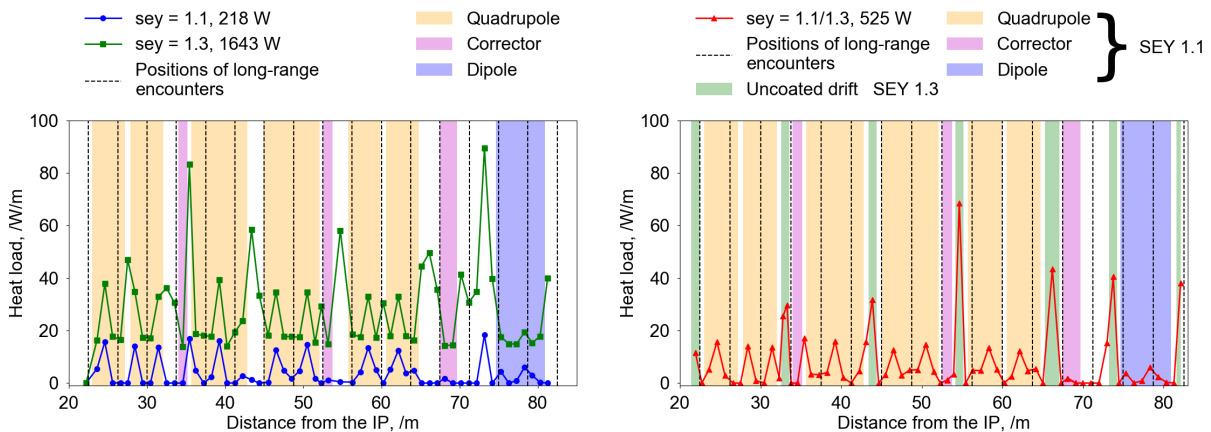


Figure 3: Heat load along one of the IR5 triplets for two uniform SEY cases (left) and a nonuniform SEY case (right) where the drift spaces outside the cold masses are not coated. The colored areas mark different magnetic field configurations as indicated in the legend.

drift sections. The heat load expected in absence of surface treatment is very high, in the order of 1.5 kW, but a strong reduction is observed when *a-C* coating is applied.

Due to technical difficulties, the coating might not be applied for some components in the drift sections located outside the cold masses, like the beam position monitors and the bellows. For this reason, the case of a non-uniform SEY along the triplet was studied, assuming that all the drifts between the cold masses are not coated and have SEY=1.3. The right plot in Fig. 3 shows the heat load distribution along the triplet under these assumptions. The uncoated drifts are indicated with the green background color. One can notice that the heat load density in these regions is significantly larger compared to the coated sections. The heat load from uncoated drifts constitutes more than a half of the total heat load in the triplet. This needs to be taken into account in the cryogenics design. More details on the e-cloud studies for the Inner Triplets of the HL-LHC can be found in [12].

### TDIS absorber

The 3D model of the TDIS absorber is shown in Fig. 2. By design it will have three segments in separate tanks, allowing for better alignment of the device with respect to the beam [13]. The jaws in the first two segments will be made of graphite, which has a low SEY parameter, close to 1.0, whereas the jaws in the third tank will be metallic with a section in aluminum coated with titanium and a section in copper.

A first set of simulation was performed assuming the same SEY parameter for all surfaces exposed to the beam. The e-cloud buildup was simulated for the different jaw configurations. It was found that the electron current is increasing with the jaw opening. The most critical half-gap size was found at about 40 mm. Similarly to the case of the Inner Triplets, the current tends to be larger at locations between LREs as can be seen in Fig. 5. Interestingly, the dependence of the e-cloud on the distance from the LREs

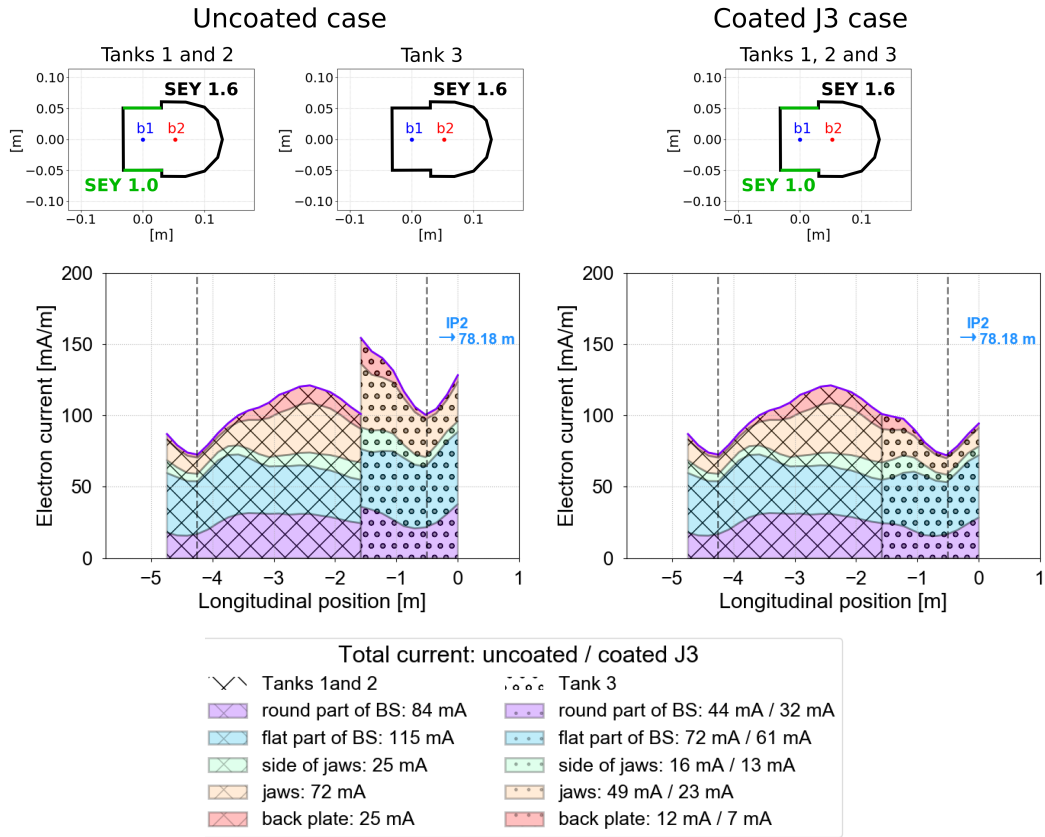


Figure 4: Contributions to the total electron current from different surfaces for the uncoated (left) and the coated (right) SEY distributions.

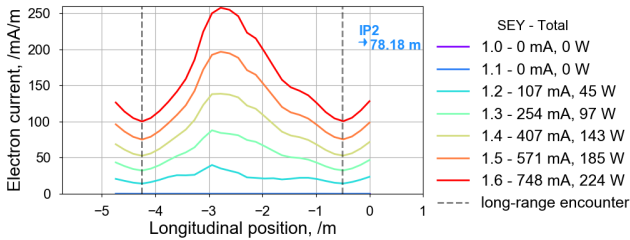


Figure 5: Longitudinal profile of the electron current in the TDIS for the 40 mm half-gap and different SEY (uniform over the chamber). The total current for each SEY is indicated in the legend. The positions of LREs are marked with dashed vertical lines.

was found to change significantly with the bunch population (for details see [8]).

More advanced simulations were performed to assess the detailed electron current distribution along the device assuming a realistic non-uniform SEY profile. We assumed SEY=1.6 for the metallic parts, corresponding to the partially conditioned surface. Since the metallic jaws in tank three are expected to have high SEY, the possibility of coating them with *a-C* was studied. Figure 4 (top) shows the SEY distributions in the TDIS chamber along the three tanks without coating and with the coating applied on the jaws in tank three (*coated J3*). The two corresponding longitudinal electron current profiles are shown in Fig. 4 (bottom). Dif-

ferent colors mark contributions from different surfaces of the chamber. The effect of *a-C* coating on the jaws in tank three is clearly visible. However, it is evident that a large contribution comes from the surface of the beam screen (blue and purple) in both cases. The portion of electrons impacting on the surface of the beam screen, including round and flat parts, constitutes more than half of the total number of electrons.

Based on these results the effect of *a-C* coating on the beam screen was also studied. The e-cloud in the TDIS was simulated assuming the SEY configuration shown in Fig. 6. Simulations have shown that if both the beam screen and the jaws in tank three are coated with *a-C* (SEY=1.0), the electron current can be fully suppressed.

The results of these simulations were used as an input for dynamic pressure studies [14]. It was shown that by suppressing the multipacting on the beam-screen the target pressure of less than  $5 \times 10^{-9}$  mbar can be achieved even without coating of the metallic jaws. More details on the e-cloud studies for the TDIS absorber can be found in [8].

## CONCLUSIONS

E-cloud build-up simulations with two beams in a common chamber require particular care. Due to the nonlinearities of the e-cloud, the single beam case cannot be simply scaled to describe the situation when multiple beams

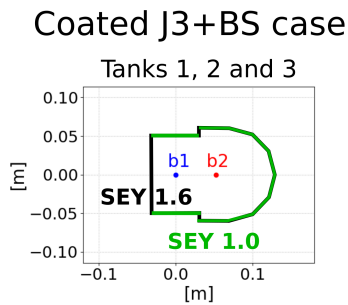


Figure 6: SEY distribution in the TDIS in the case when a-C coating is applied to both the jaws in tank three and the beam screen.

are present in one chamber. The dependence on the location due to changing hybrid bunch spacing along the device needs to be taken into account.

The e-cloud build-up was studied in the main elements of the Inner Triplets of the HL-LHC considering different coating scenarios. Simulations have shown that if all the triplet elements will be coated with a-C except for the drifts between the cold masses, the total heat load could be reduced by factor of three.

E-cloud build-up simulations for the TDIS absorber have shown that the a-C coating can significantly reduce the electron current. Most of the electrons were found to be produced on the beam screen surface. Simulations with a-C applied on both the metallic jaws and the beam screen have shown that the e-cloud in this scenario can be fully suppressed.

## ACKNOWLEDGEMENTS

Authors would like to thank C. Bracco, R. De Maria, P. Dijkstal, L. Gentini, G. Mazzacano, A. Perillo-Marcone, P. Ribes Metidieri, A. Romano, G. Rumolo, M. Taborelli and C. Yin-Vallgren for their valuable input. Research supported by the HL-LHC project.

## REFERENCES

- [1] G. Iadarola, G. Rumolo, P. Dijkstal, and L. Mether, "Analysis of the beam induced heat loads on the LHC arc beam screens during Run 2," December 2017, CERN (CERN-ACC-NOTE-2017-0066).
- [2] G. Iadarola, "Digesting the LIU high brightness beam: is this an issue for HL-LHC?", unpublished. Presentation at the LHC Performance Workshop 2018, 31 January 2018, Chamonix.
- [3] G. Apollinari *et al.*, "High-Luminosity Large Hadron Collider (HL-LHC): Technical Design Report V. 0.1". CERN Yellow Reports: Monographs 4/2017, Geneva: CERN,2017.
- [4] "PyE-CLOUD code"  
<https://github.com/PyCOMPLETE/PyE-CLOUD/wiki>
- [5] G. Iadarola, "Electron Cloud Studies for CERN Particle Accelerators and Simulation Code Development", CERN-THESIS-2014-047, March 2014.
- [6] F. Zimmermann, "Electron-cloud Simulations for the LHC Straight Sections," LHC-PROJECT-NOTE-201, Geneva, CERN, 1999.
- [7] A. Rossi *et al.*, "A simulation study of the electron cloud in the experimental regions of the LHC", in Proc. 8th European Particle Accelerator Conference, Paris, France, 3 - 7 Jun 2002, pp.2583.
- [8] G. Skripka, G. Iadarola, "Electron cloud studies for the LHC TDI and HL-LHC TDIS", August 2018, CERN (CERN-ACC-NOTE-2018-0060).
- [9] D. Carbajo Perez *et al.*, "Operational Feedback and Analysis of Current and Future Designs of the Injection Protection Absorbers in the Large Hadron Collider at CERN", in Proceedings of the 8th International Particle Accelerator Conference (IPAC 2017): Copenhagen, Denmark, May 14-19, 2017, 2017 (WEPVA108).
- [10] A. Lechner *et al.*, "TDI - Past observations and improvements for 2016", in Proceedings of the 2015 Evian Workshop on LHC beam operation, p. 123, September 2015.
- [11] A. Lechner, "Summary of issues with the present TDI – the TDI history in a nutshell", unpublished. Presented at TDIS Internal Review Meeting 2016, CERN, 2016.
- [12] G. Skripka, G. Iadarola, "Beam-induced heat loads on the beam screens of the inner triplets for the HL-LHC", February 2018, CERN (CERN-ACC-NOTE-2018-0009).
- [13] L. Gentini, "Updates on detailed TDIS mechanical design", unpublished. Presented at WP14 Coordination meeting: TDIS updates, D1 FLUKA calculations, CERN, 2017.
- [14] P. Ribes Metidieri *et al.*, "TDIS pressure profile simulations after LS2", CERN-ACC-NOTE-2018-0075.